The folding equilibria of enterobactin enantiomers and their interaction with actinides

Ziyi Liu[1,2], Zhifang Chai[1,3], and Dongqi Wang[1,*]

[1]Multidisciplinary Initiative Center, Institute of High Energy Physics, Chinese Academy of Sciences, Beijing, 100049

[2]University of Chinese Academy of Sciences, Beijing, 100049
[3]School of Radiation Medicine and Interdisciplinary Sciences (RAD-X), Soochow University, Suzhou, Jiangsu, 215123

Electronic Supplementary Information:

1. RMSF

Table S1. The root mean square fluctuation (RMSF) of heavy atoms of Ent(S) and Ent(R) during $M^{3+/4+}$-Ent MD simulations. (unit: nm)

$An^{3+/4+}$	RMSF
Fe^{3+}	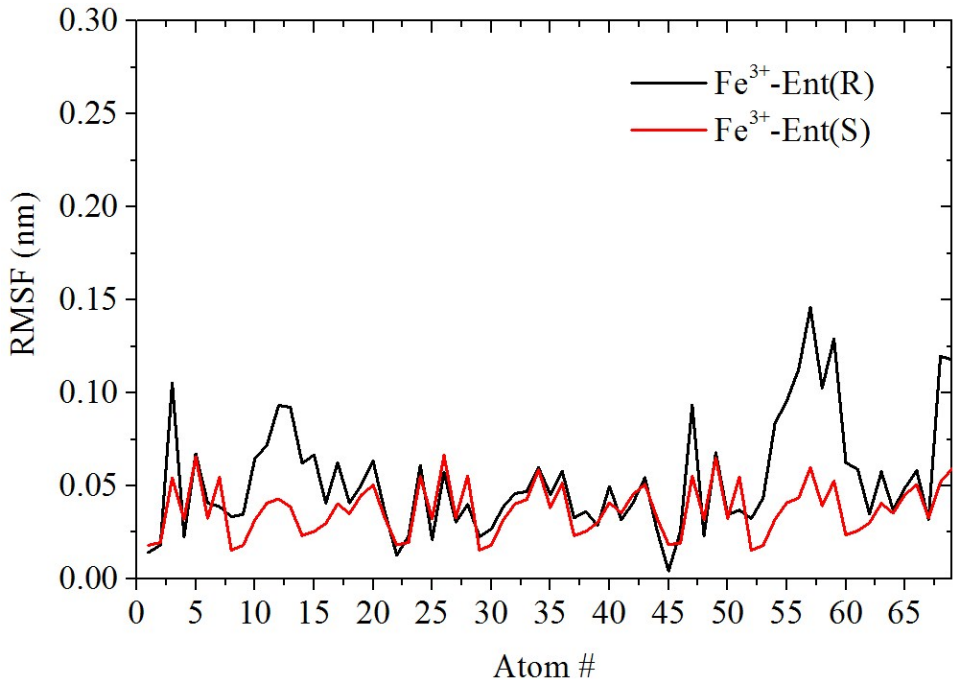

Am^{3+}	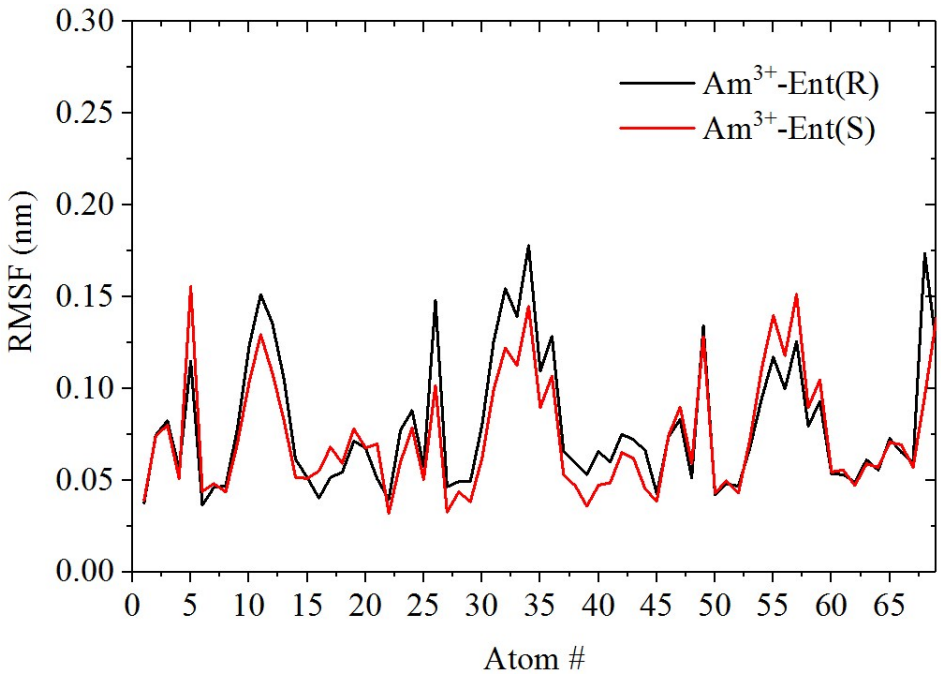 Am3+-Ent(R) Am3+-Ent(S) RMSF (nm) Atom # 0.00 0.05 0.10 0.15 0.20 0.25 0.30 0 5 10 15 20 25 30 35 40 45 50 55 60 65
Cm^{3+}	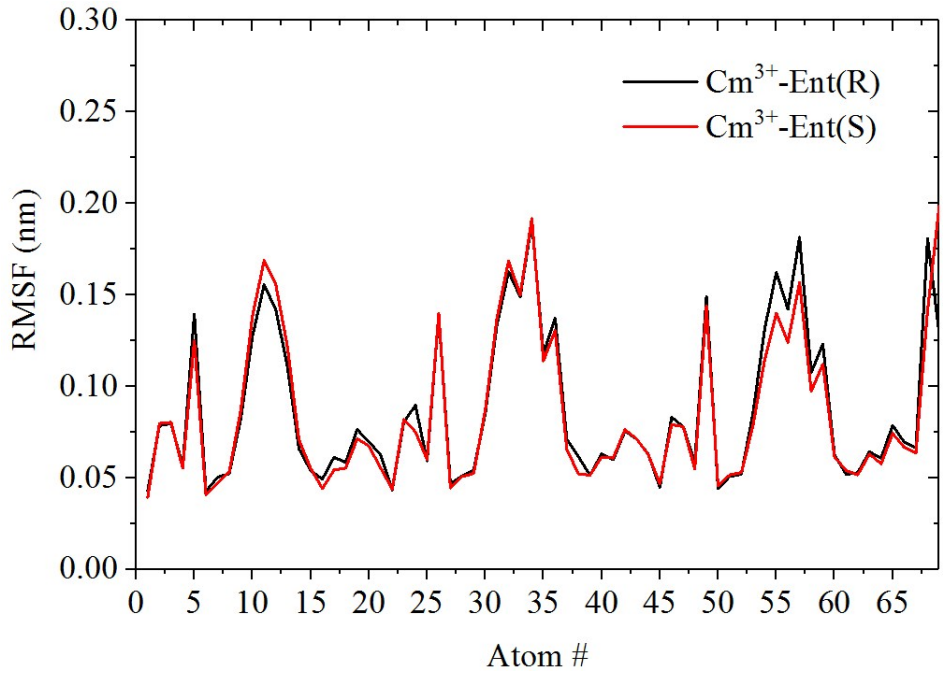 Cm3+-Ent(R) Cm3+-Ent(S) RMSF (nm) Atom # 0.00 0.05 0.10 0.15 0.20 0.25 0.30 0 5 10 15 20 25 30 35 40 45 50 55 60 65

Th^{4+}	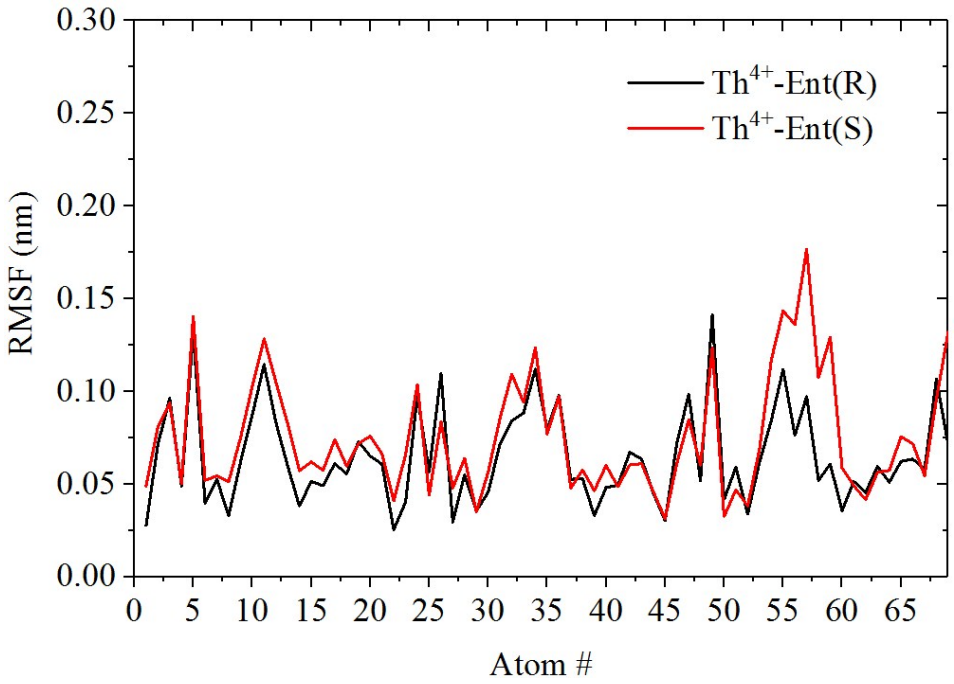 Th4+-Ent(R) Th4+-Ent(S) RMSF (nm) Atom # 0.00 0.05 0.10 0.15 0.20 0.25 0.30 0 5 10 15 20 25 30 35 40 45 50 55 60 65
U^{4+}	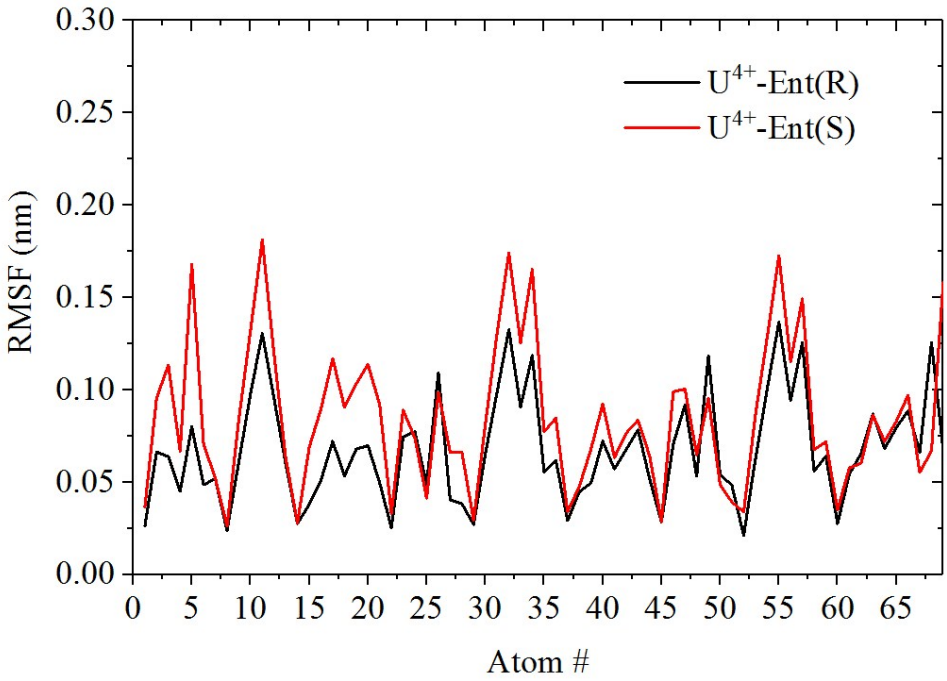 U4+-Ent(R) U4+-Ent(S) RMSF (nm) Atom # 0.00 0.05 0.10 0.15 0.20 0.25 0.30 0 5 10 15 20 25 30 35 40 45 50 55 60 65

Np^{4+}	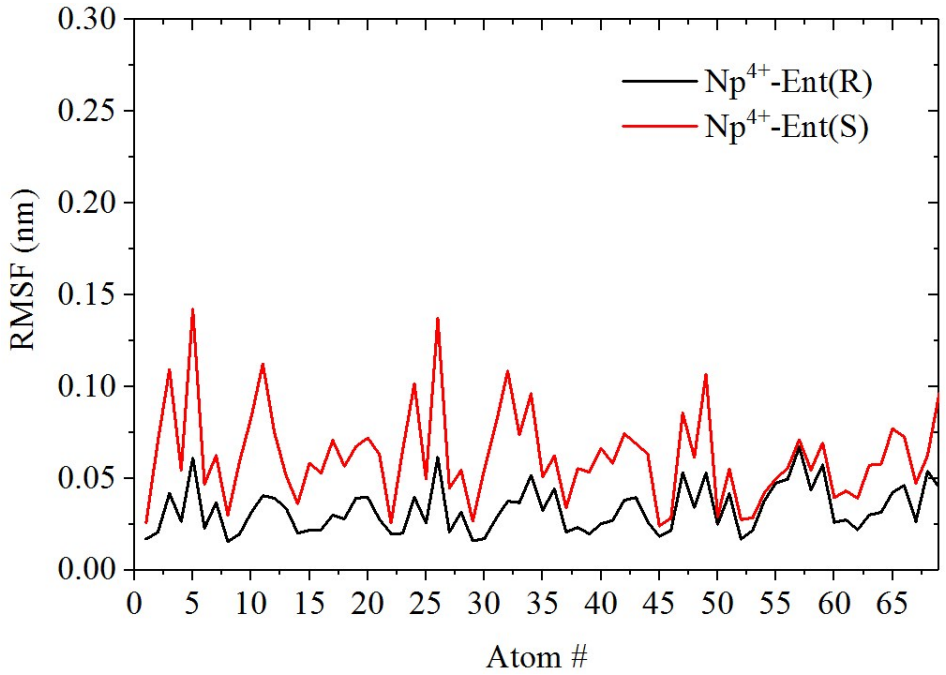 Np4+-Ent(R) Np4+-Ent(S) RMSF (nm) Atom #
Pu^{4+}	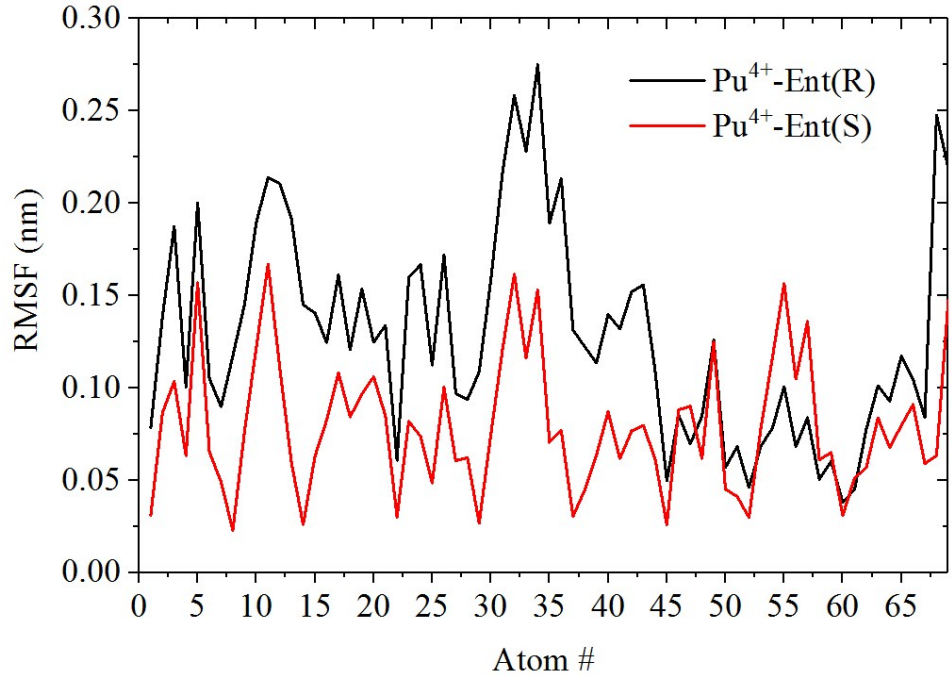 Pu4+-Ent(R) Pu4+-Ent(S) RMSF (nm) Atom #

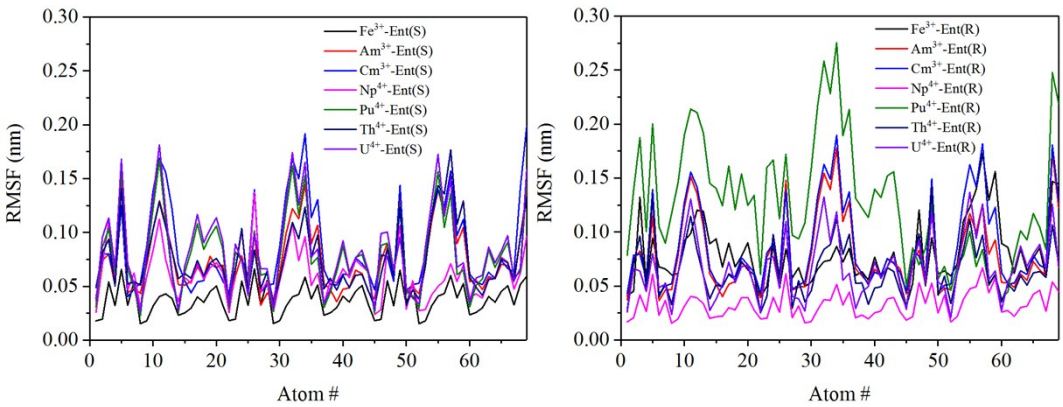

Figure S1. The root mean square fluctuation (RMSF) of heavy atoms of Ent(S) and Ent(R) during $M^{3+/4+}$-Ent MD simulations. (unit: nm)

2. Interaction interface of water and aromatic ring

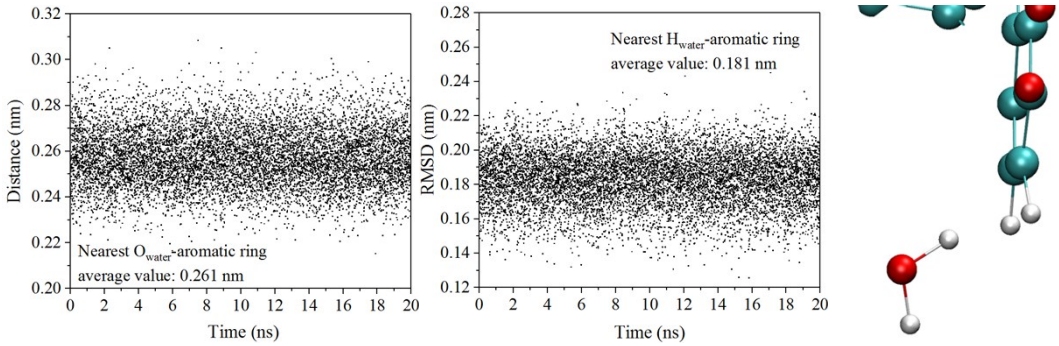

Figure S2. The distance between nearest O_{water} (**left**) / H_{water} (**middle**) and aromatic ring atoms of catechol during the dynamics, and their average value is marked. A snapshot of interaction model is represented (**right**). (unit: nm)

3. RDF

Table S2. Radial distribution functions (RDF) of O_{Ent} (O_o: black; O_i: red) and O_{water} (bottom) around metal ion (Fe^{3+}, Am^{3+}, Cm^{3+}, Th^{4+}, U^{4+}, Np^{4+}, Pu^{4+}) and the corresponding integrals (dotted lines). (unit: nm)

		Ent(S)	Ent(R)
Fe^{3+}	O_{Ent}	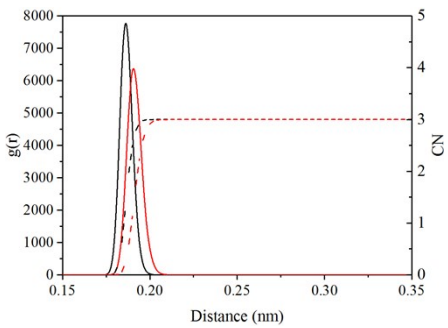	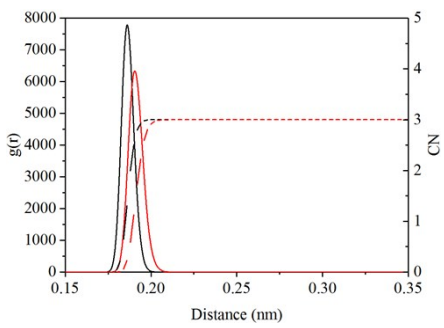

	O_{water}	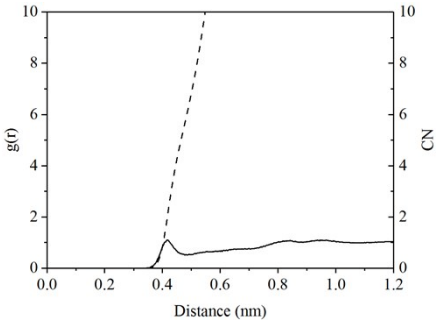	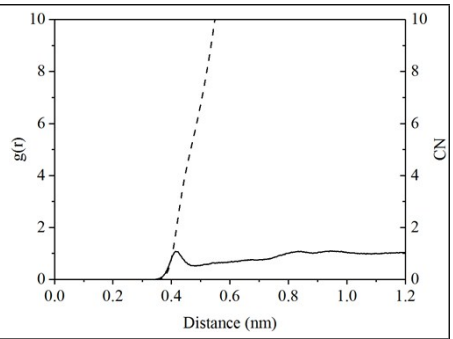
Am^{3+}	O_{Ent}	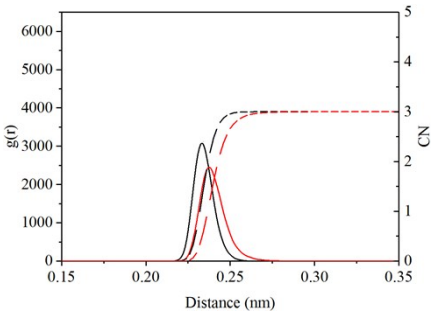	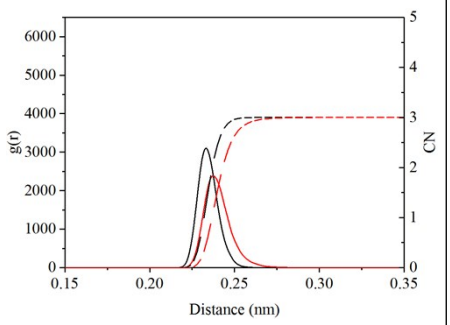
	O_{water}	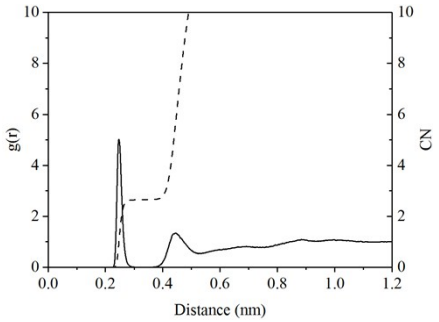	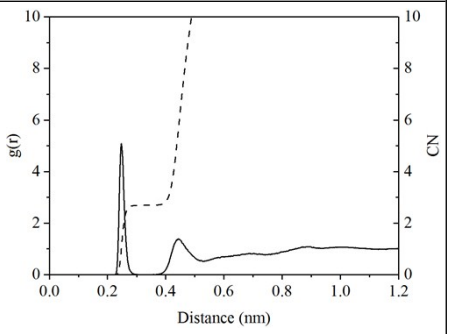
Cm^{3+}	O_{Ent}	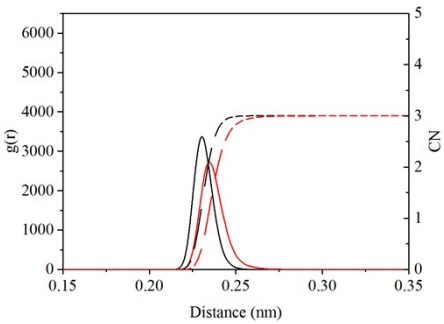	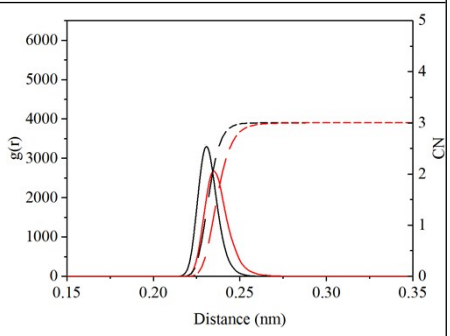
	O_{water}	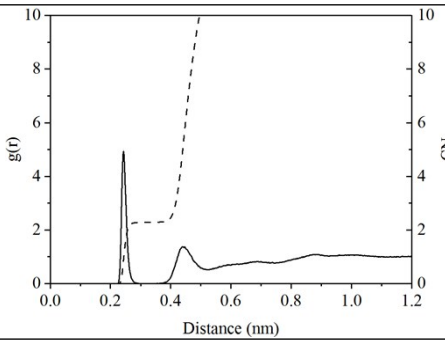	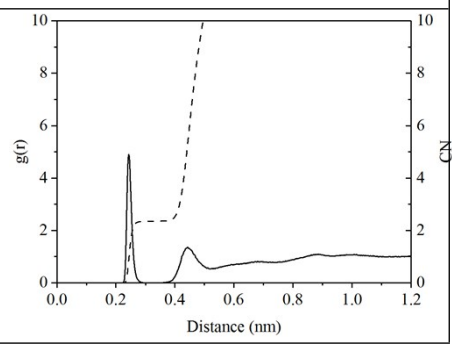

Th^{4+}	O_{Ent}	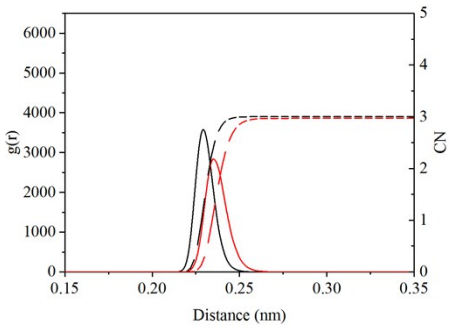	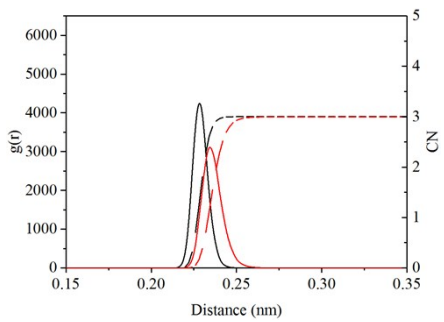
	O_{water}	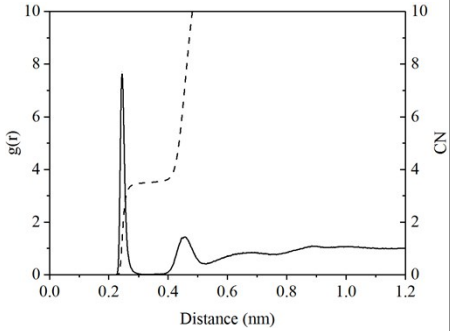	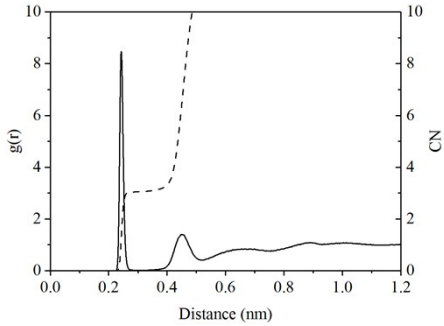
U^{4+}	O_{Ent}	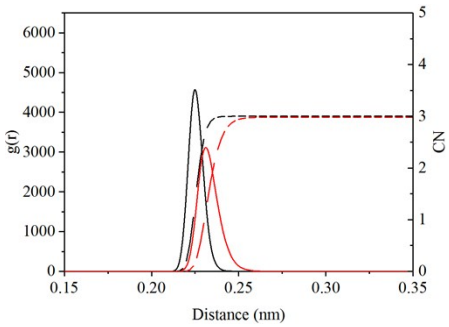	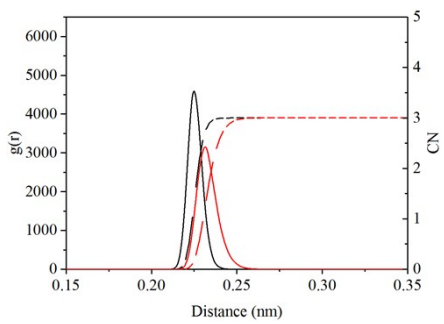
	O_{water}	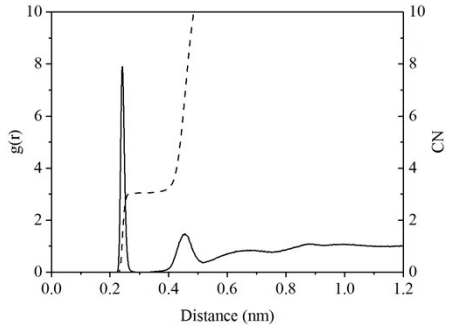	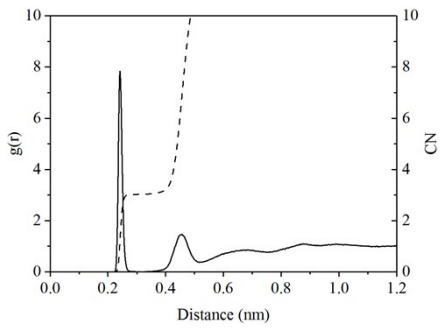
Np^{4+}	O_{Ent}	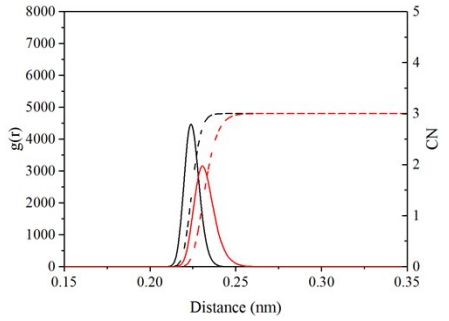	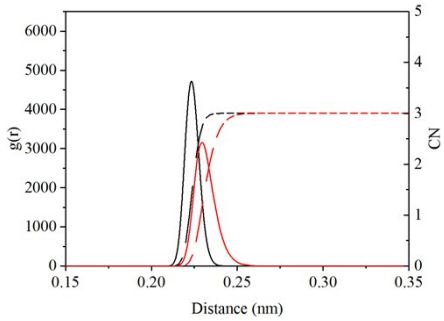

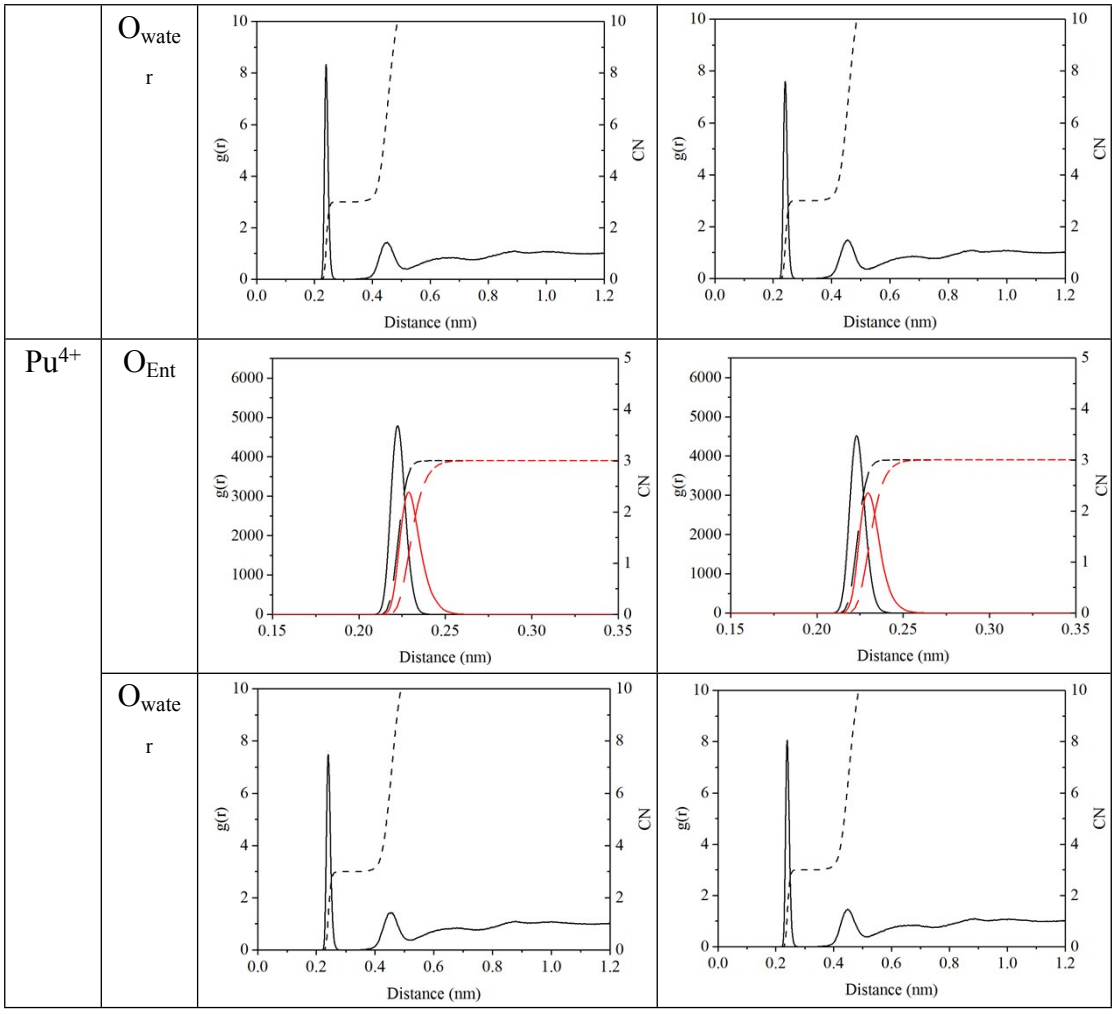

4. H-bond lifetime

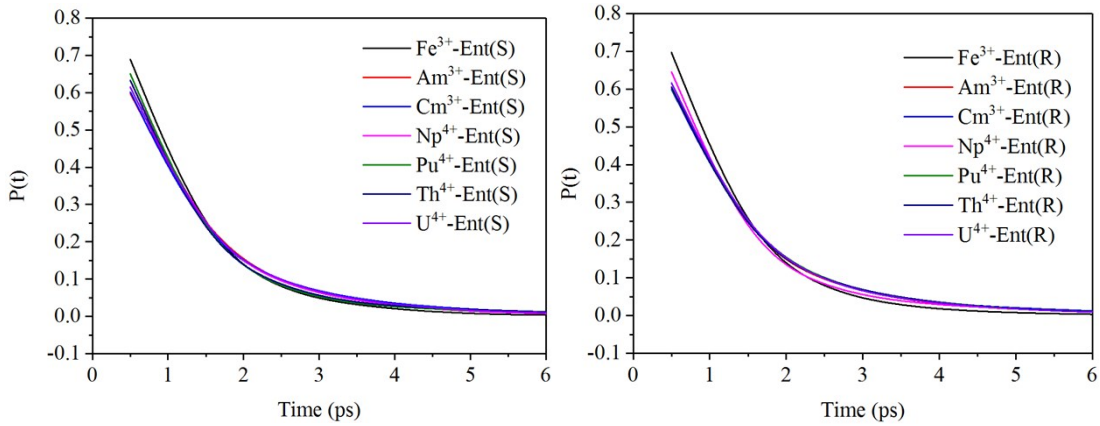

Figure S3. The lifetime of H-bond between Ent and water in $M^{3+/4+}$-Ent(S) (**left**) and $M^{3+/4+}$-Ent(R) (**right**) MD simulations.

5. Ramachandran plot

Table S3. Ramachandran map of Ent(S, R) complexes with Fe^{3+}, An^{3+} and An^{4+}. The maps are similar for the three (φ_i, ψ_i) pairs of the serine linker in each complex, and only the (φ_A, ψ_A) pairs are shown for simplicity.

	Ent(S)	Ent(R)
Fe^{3+}	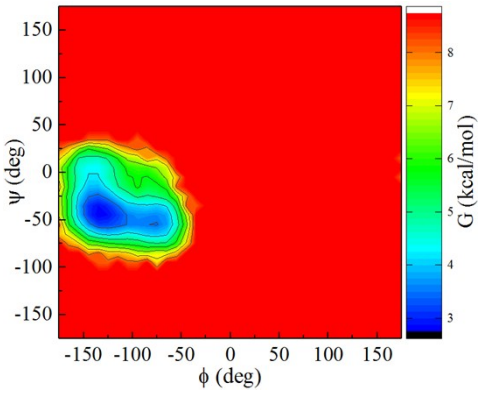	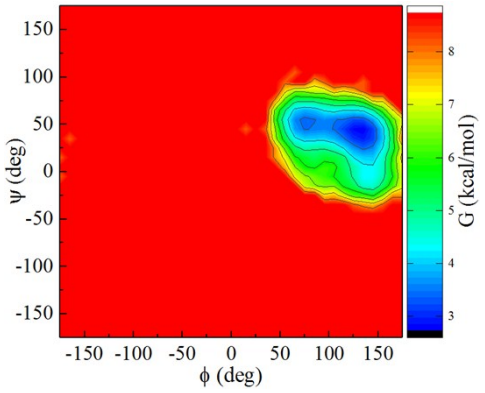
Am^{3+}	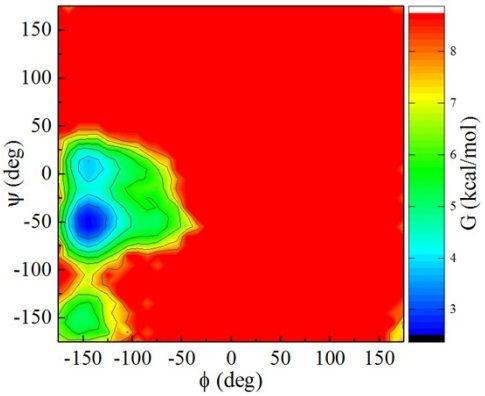	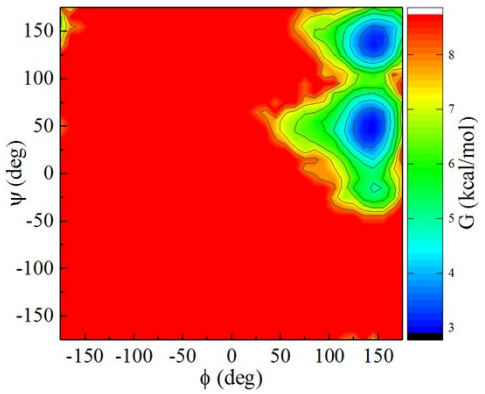
Cm^{3+}	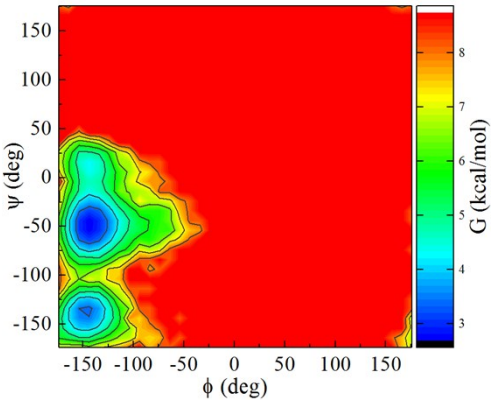	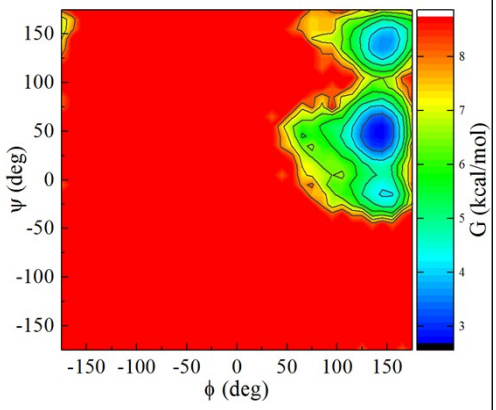
Th^{4+}	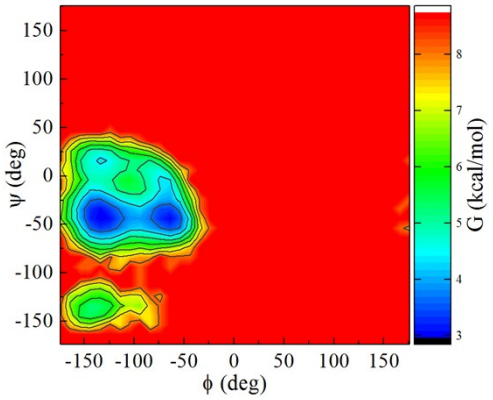	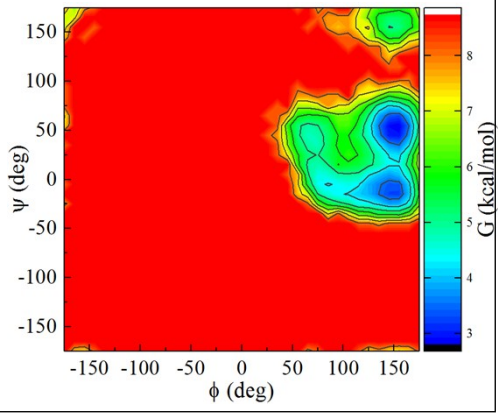

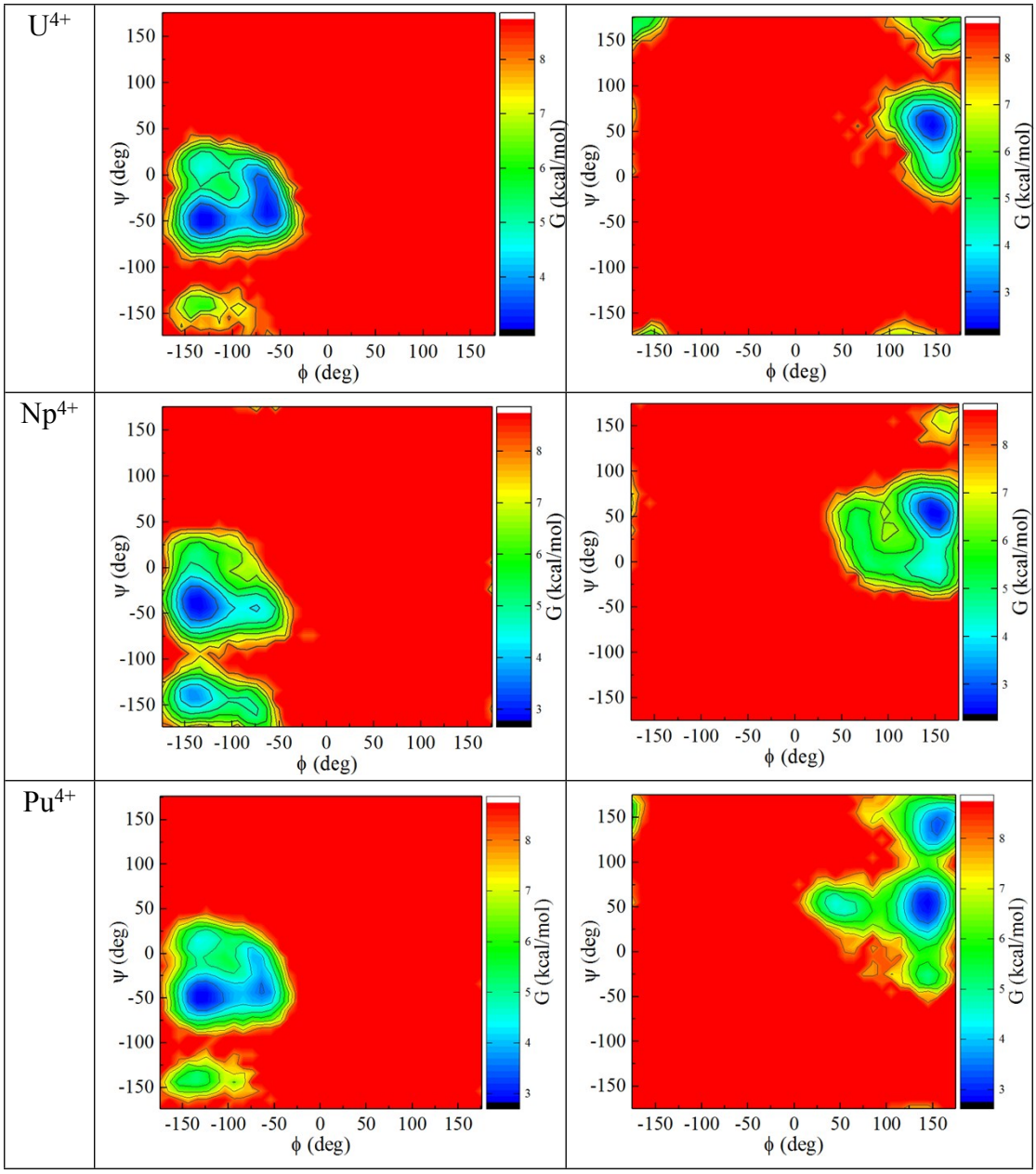

6. ϕ / ψ time evolution

Table S4. Each φ, ψ change with time evolution in $An^{3+/4+}$-Ent(S) complex during MD simulations.

		Ent(S)	
		ϕ	ψ

Fe^{3+}	1	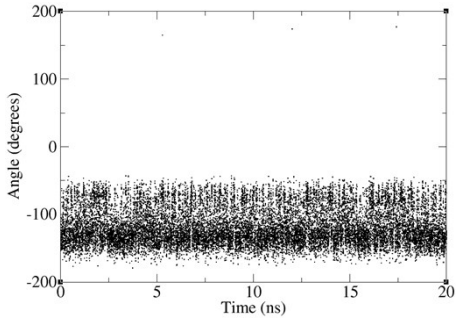	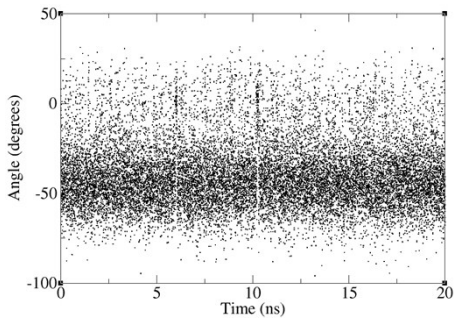
	2	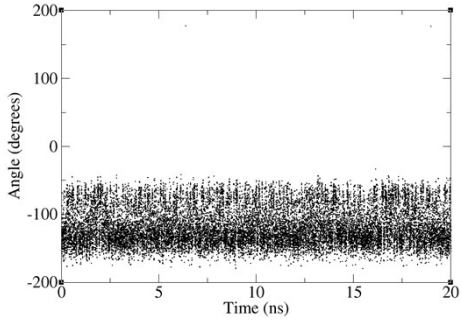	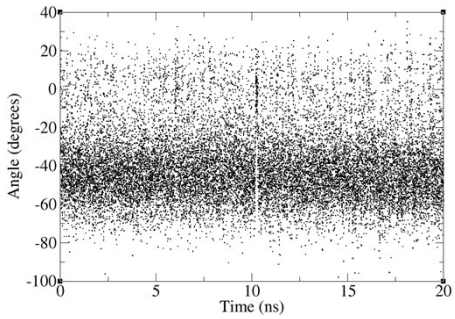
	3	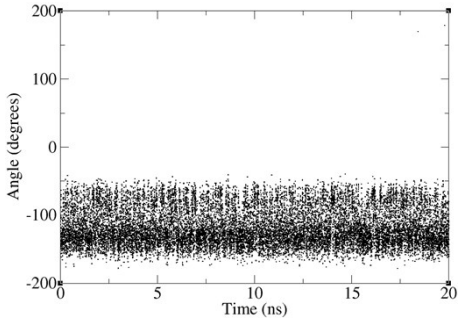	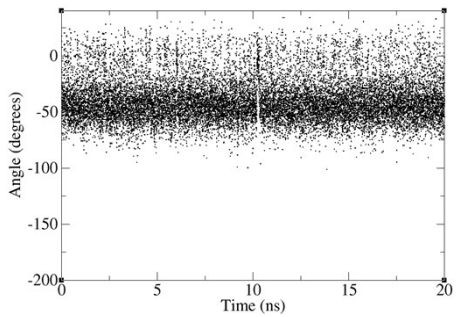
Am^{3+}	1	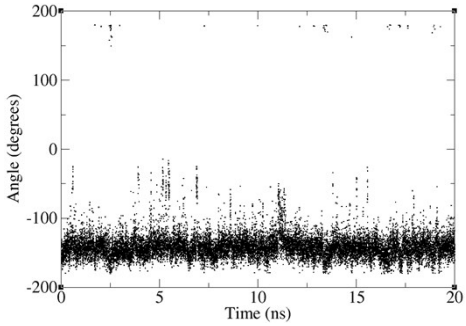	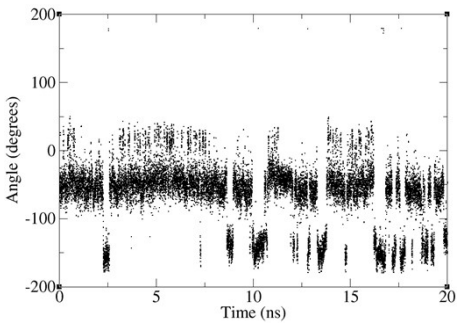
	2	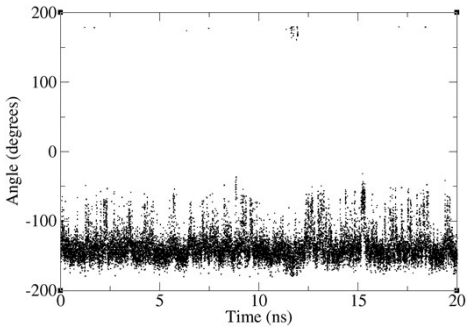	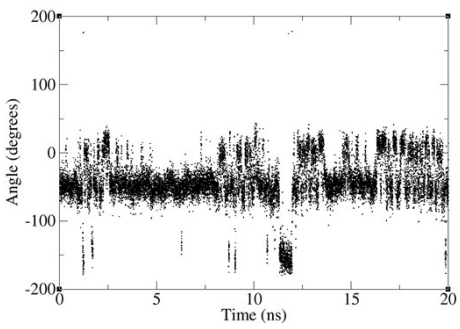

	3	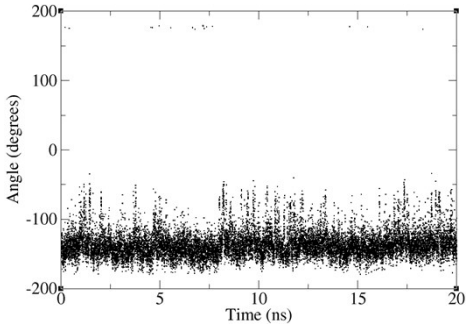	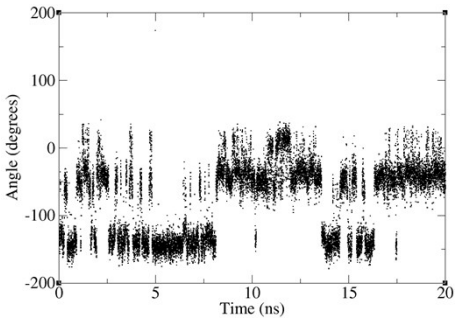
Cm^{3+}	1	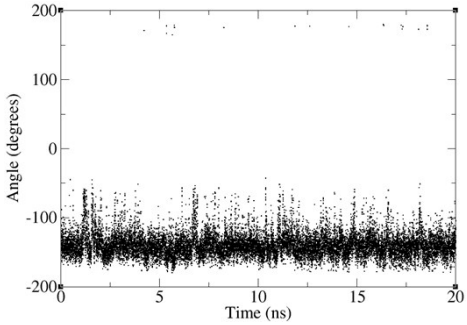	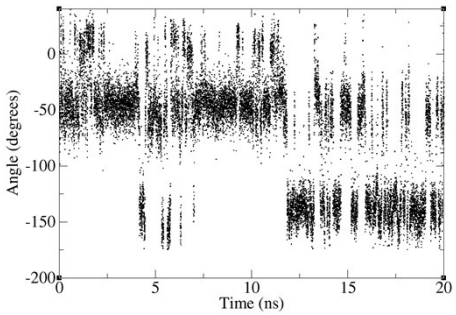
	2	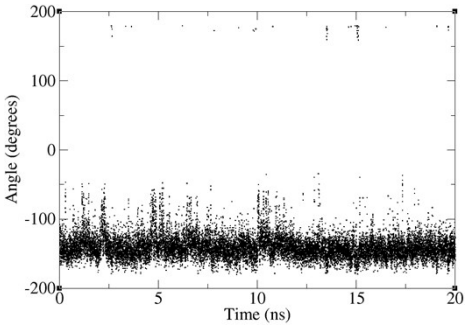	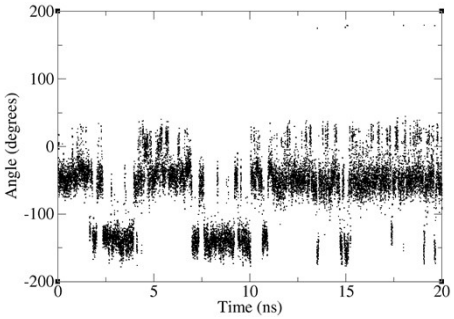
	3	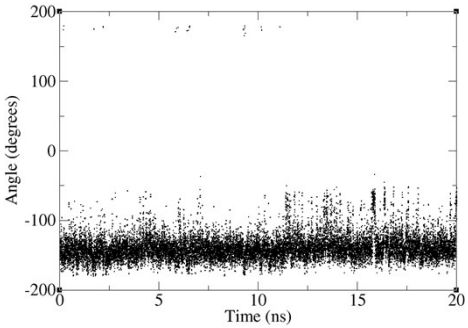	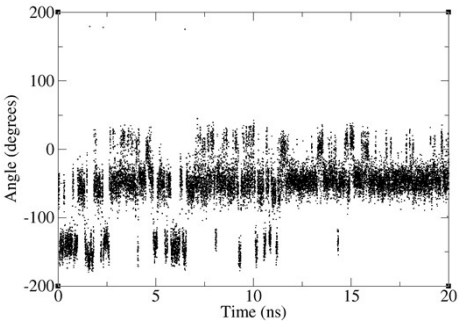
Th^{4+}	1	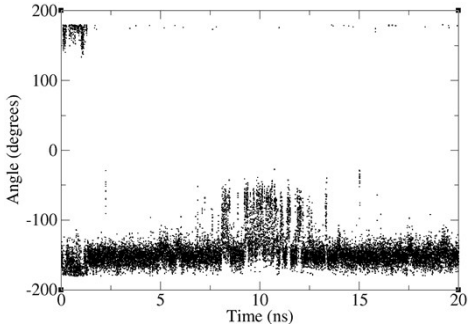	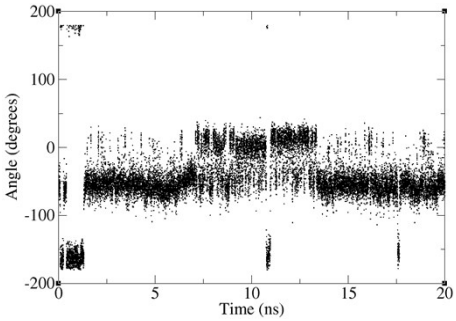

	2	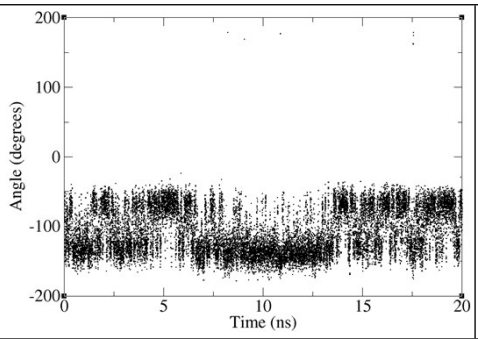 Angle (degrees) Time (ns)	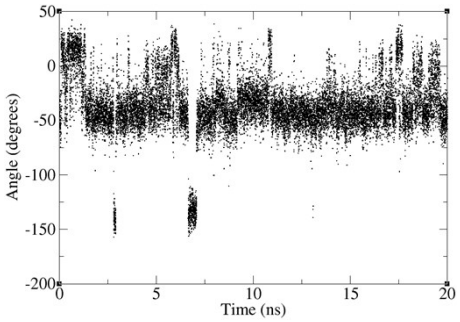 Angle (degrees) Time (ns)
	3	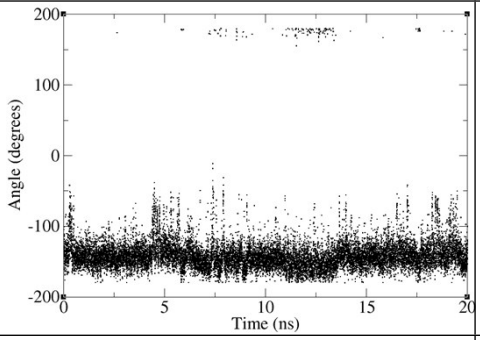 Angle (degrees) Time (ns)	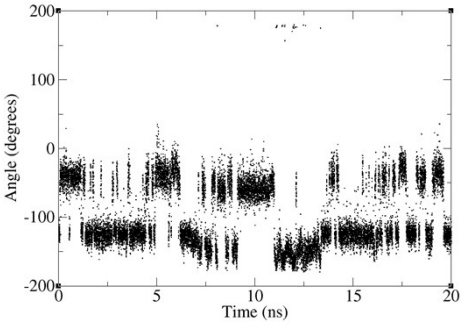 Angle (degrees) Time (ns)
U^{4+}	1	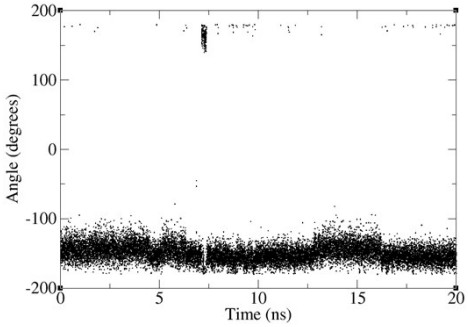 Angle (degrees) Time (ns)	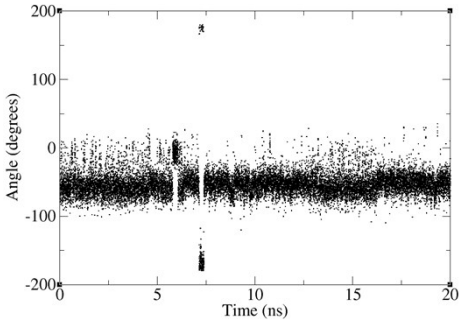 Angle (degrees) Time (ns)
	2	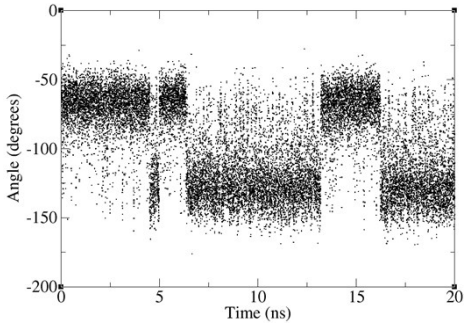 Angle (degrees) Time (ns)	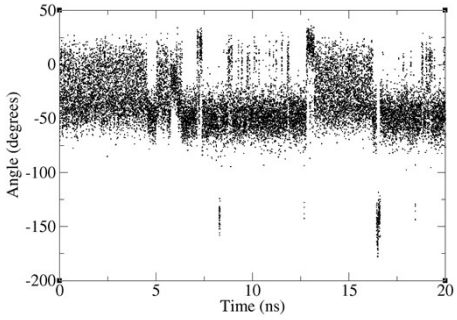 Angle (degrees) Time (ns)
	3	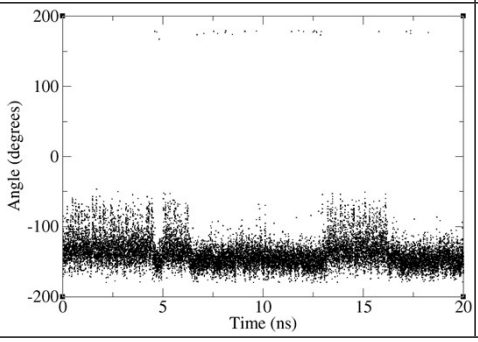 Angle (degrees) Time (ns)	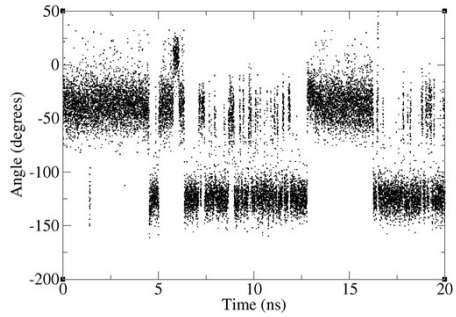 Angle (degrees) Time (ns)

Np^{4+}	1	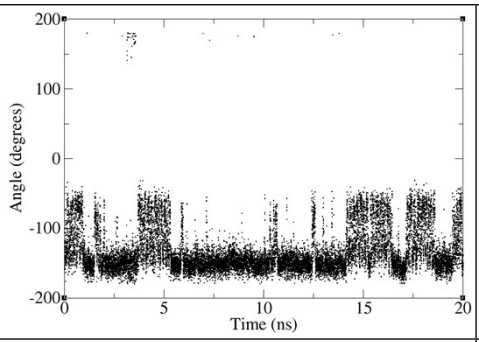	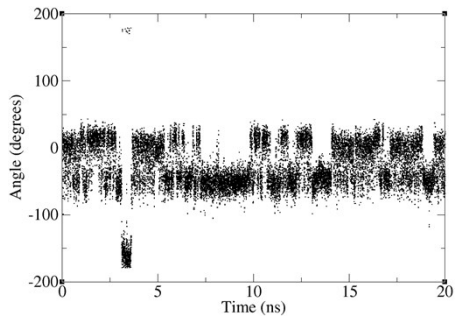
	2	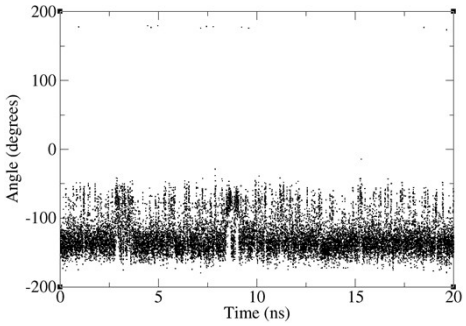	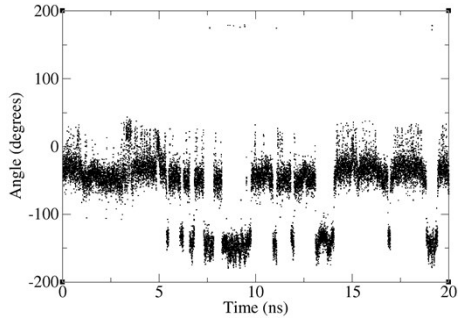
	3	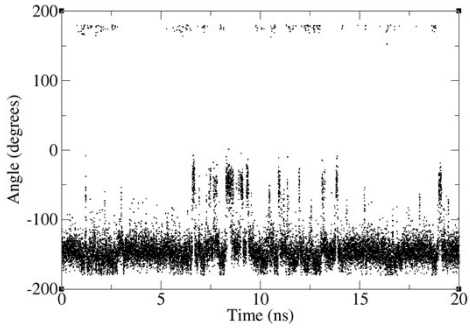	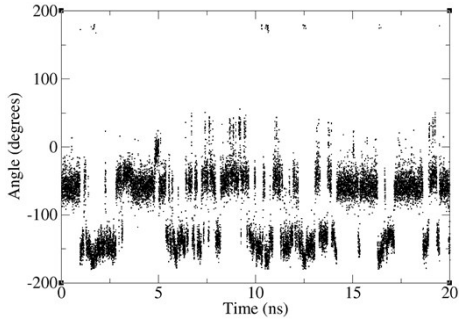
Pu^{4+}	1	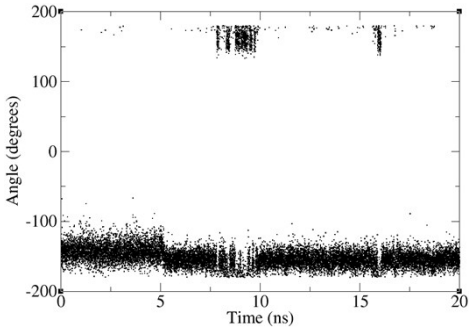	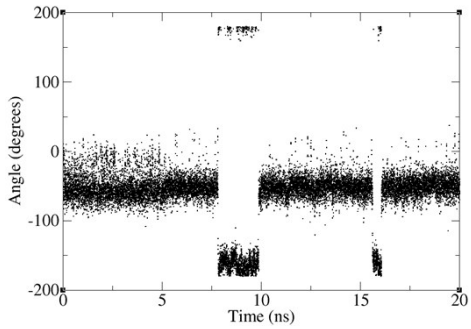
	2	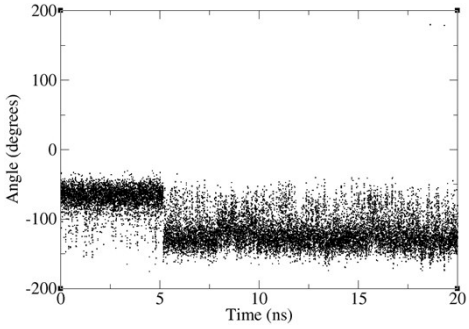	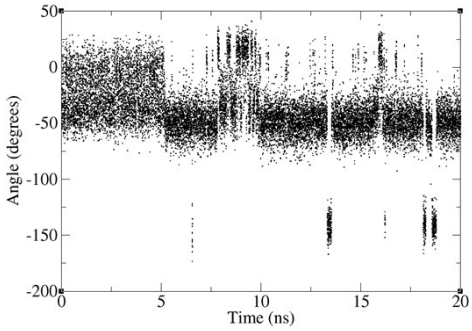

	3	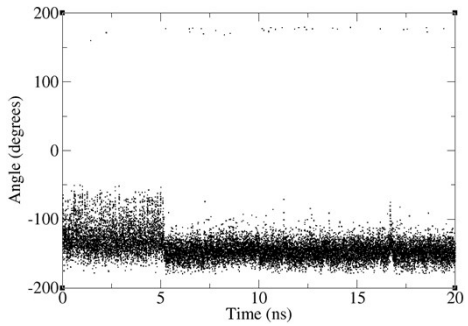	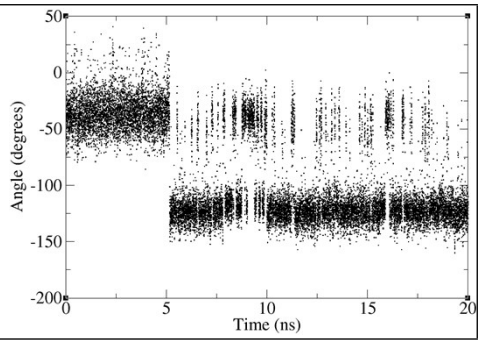

Table S5. Each φ, ψ change with time evolution in $An^{3+/4+}$-Ent(R) complex during MD simulations.

		Ent(R)	
		ϕ	ψ
Fe^{3+}	1	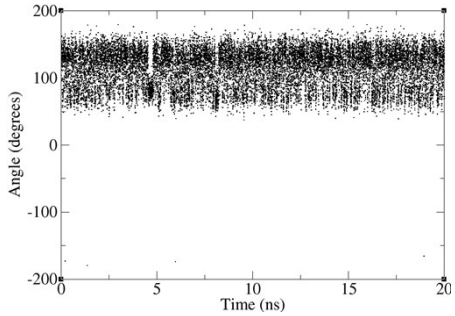	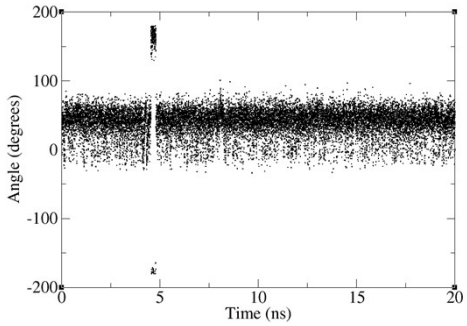
	2	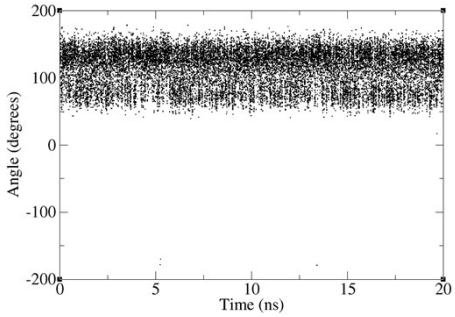	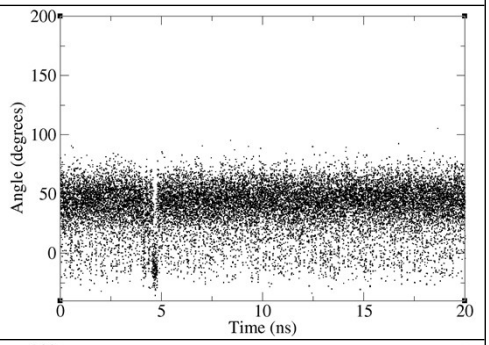
	3	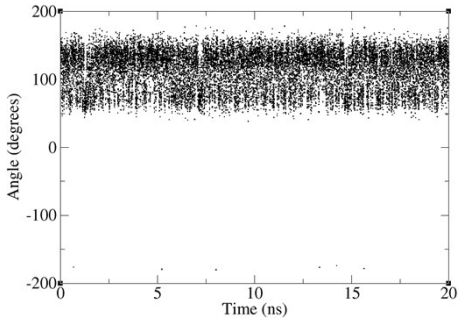	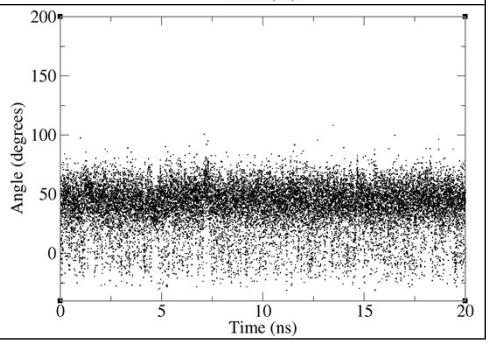

Am^{3+}	1	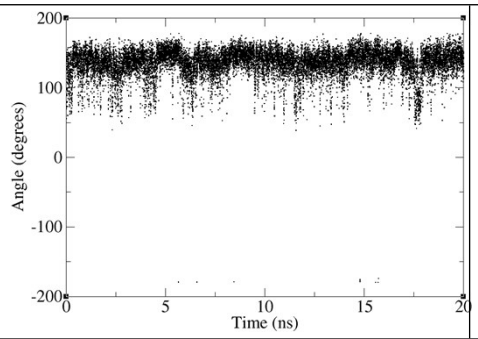	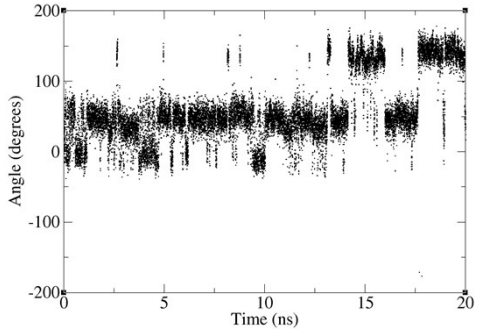
	2	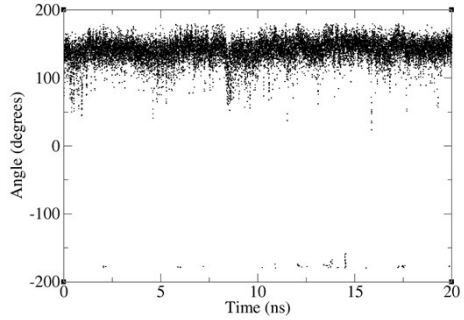	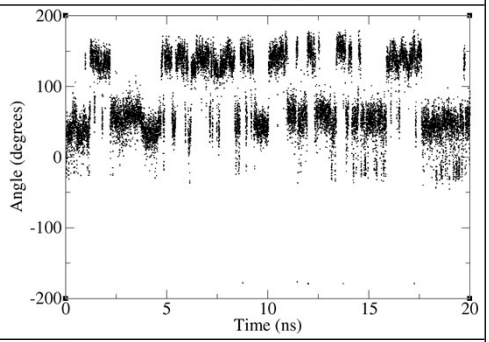
	3	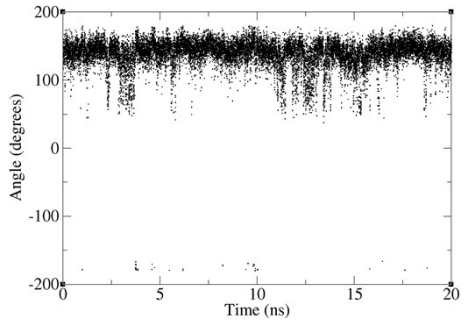	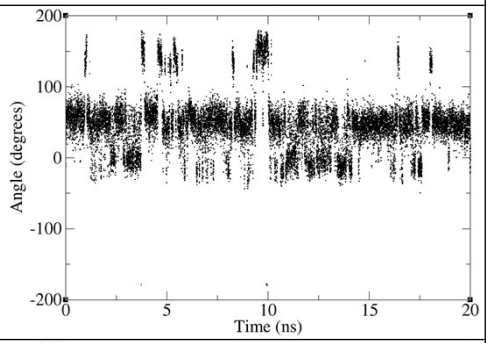
Cm^{3+}	1	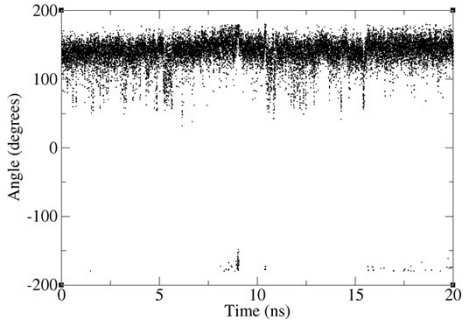	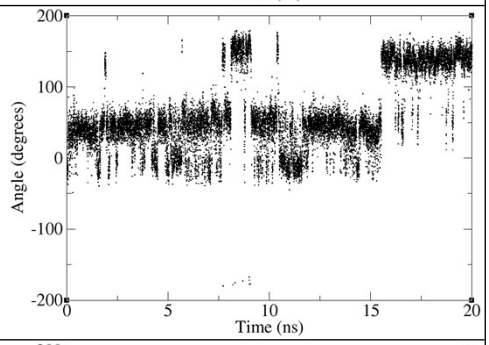
	2	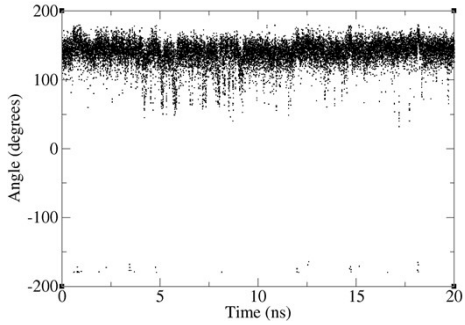	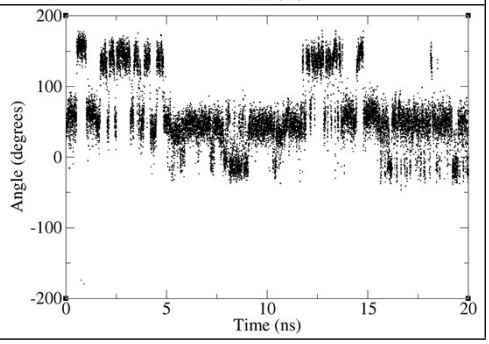

	3	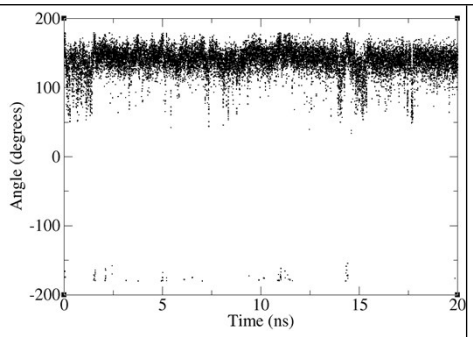 Angle (degrees) Time (ns)	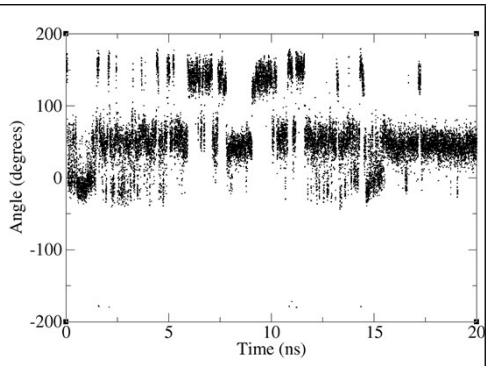 Angle (degrees) Time (ns)
Th^{4+}	1	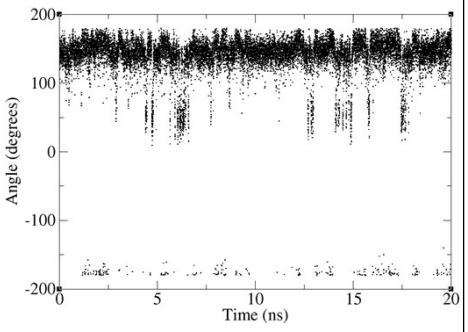 Angle (degrees) Time (ns)	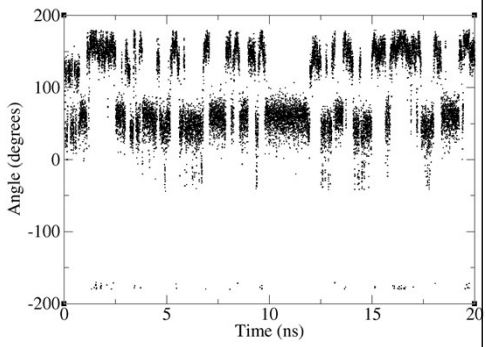 Angle (degrees) Time (ns)
	2	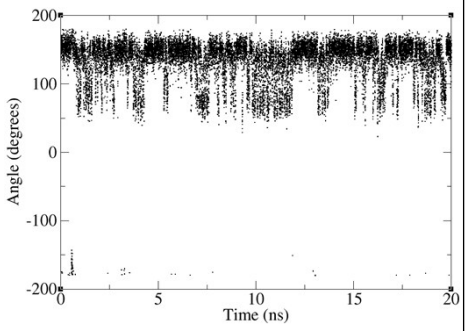 Angle (degrees) Time (ns)	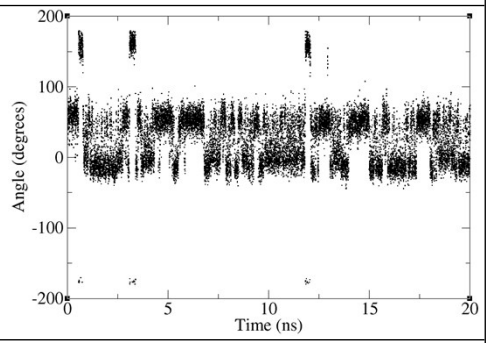 Angle (degrees) Time (ns)
	3	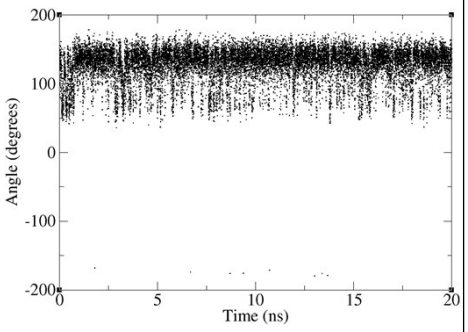 Angle (degrees) Time (ns)	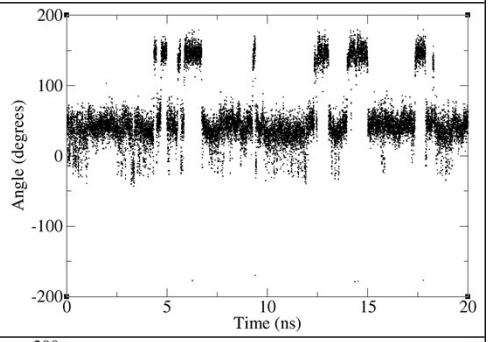 Angle (degrees) Time (ns)
U^{4+}	1	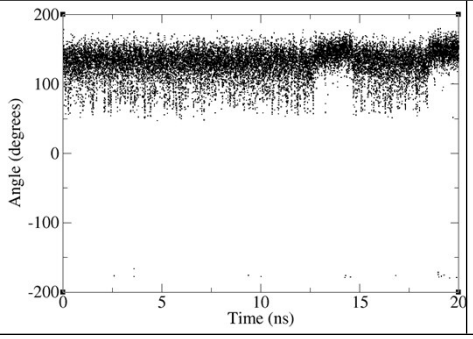 Angle (degrees) Time (ns)	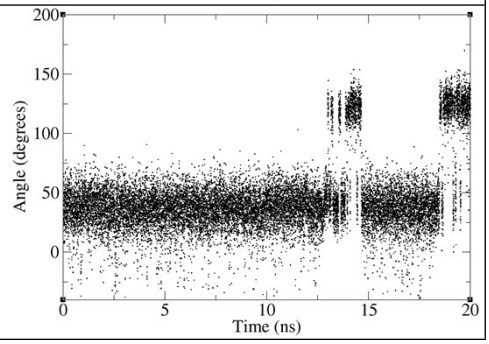 Angle (degrees) Time (ns)

	2	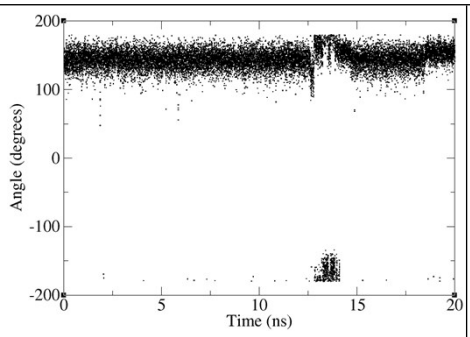 Angle (degrees) Time (ns)	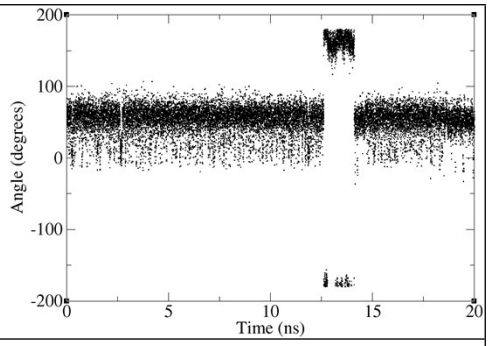 Angle (degrees) Time (ns)
	3	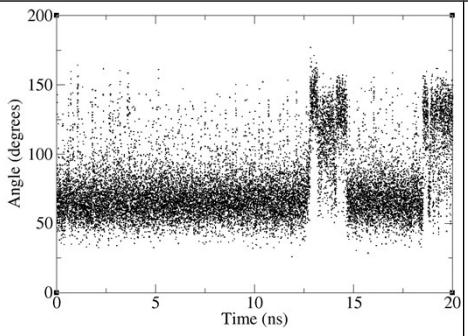 Angle (degrees) Time (ns)	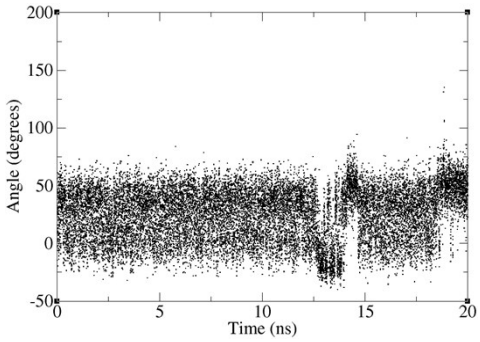 Angle (degrees) Time (ns)
Np^{4+}	1	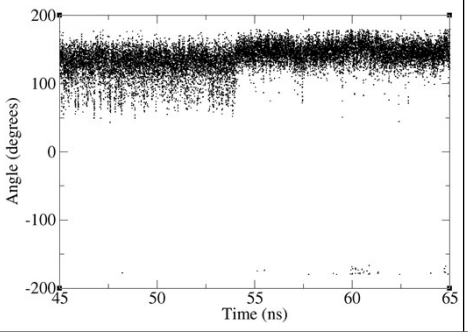 Angle (degrees) Time (ns)	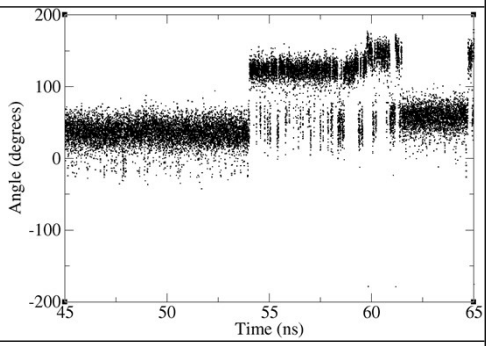 Angle (degrees) Time (ns)
	2	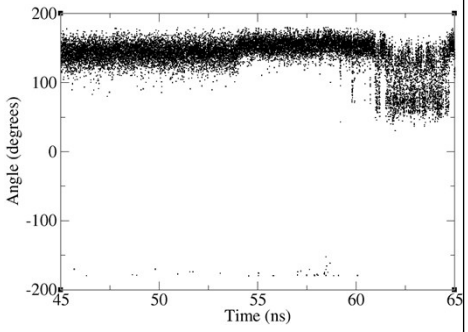 Angle (degrees) Time (ns)	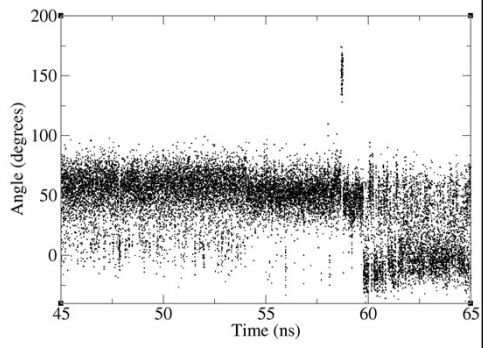 Angle (degrees) Time (ns)
	3	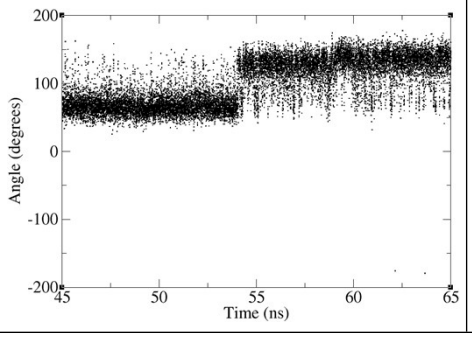 Angle (degrees) Time (ns)	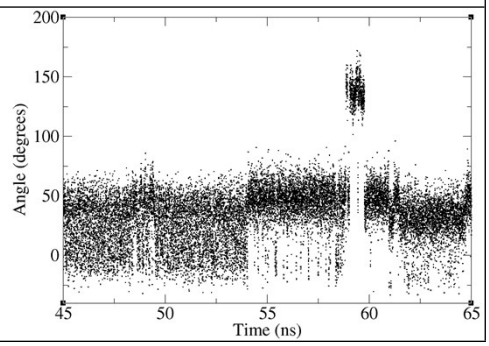 Angle (degrees) Time (ns)

Pu^{4+}	1	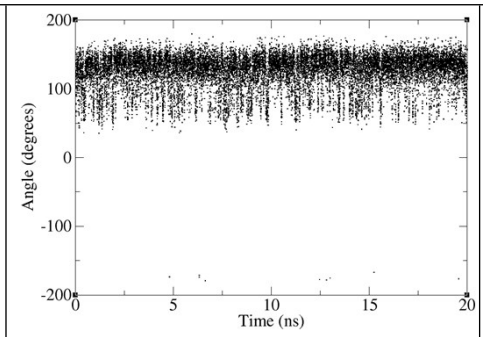	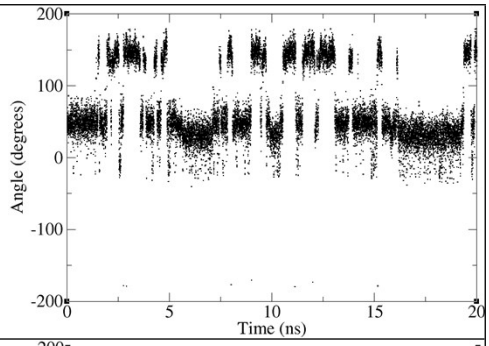
	2	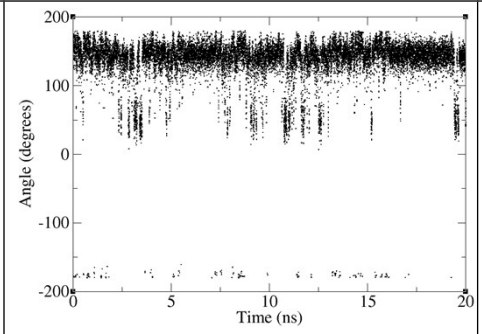	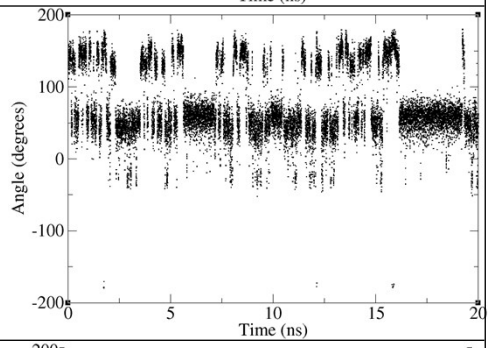
	3	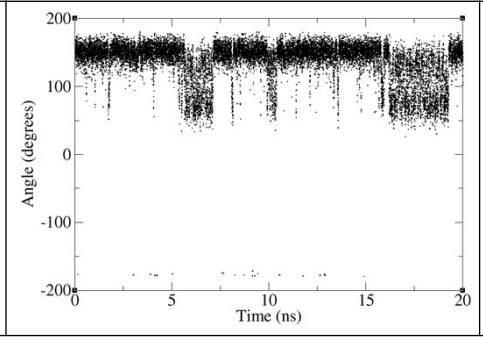	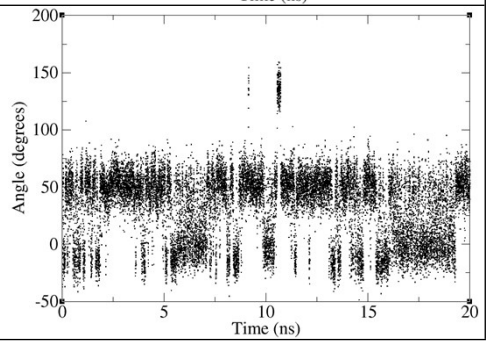

7. RMSD for Cm^{3+}, Th^{4+}, Np^{4+}-Ent complex

Table S6. Time evolution of positional RMSD of non-hydrogen atoms of Cm^{3+}, Th^{4+}, Np^{4+}-Ent(S) **(left)** and $M^{3+/4+}$-Ent(R) (**right**) complexes. The trajectories were colored to show the transitions between conformation clusters according to clustering analysis. The color scheme is according to the rank of the clusters: black, red, blue, purple and green.

	Ent(S)	Ent(R)
Cm^{3+}	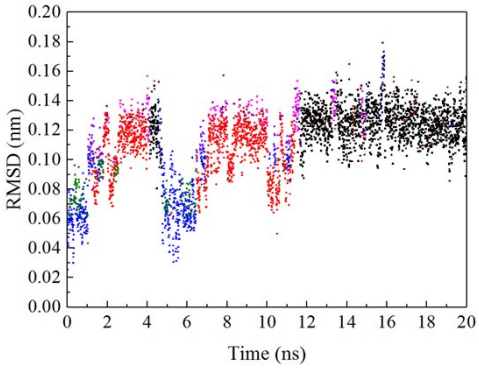	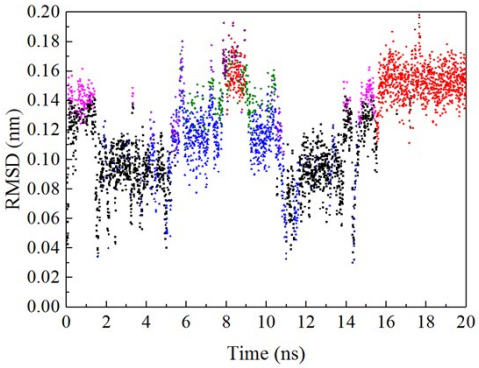

Th^{4+}	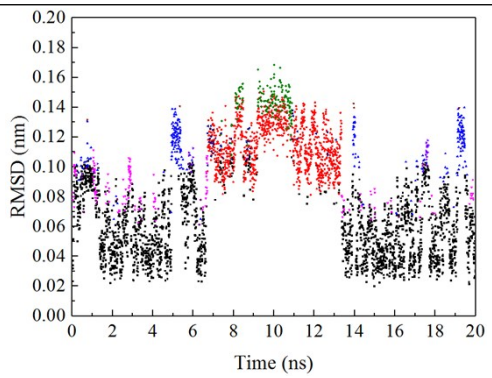	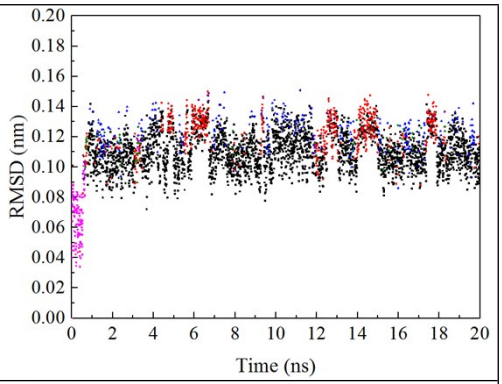
Np^{4+}	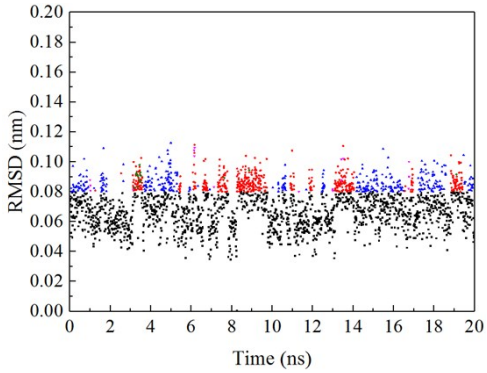	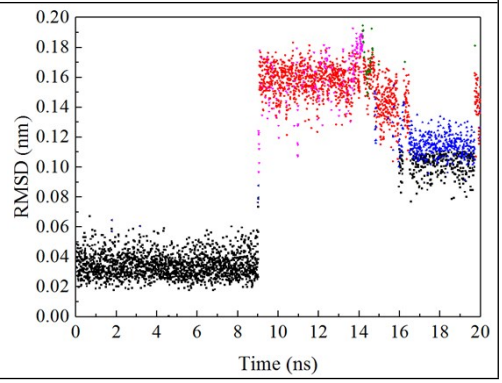

8. Polyhedral structures of metal coordination compounds

Table S7. The schematic, geometric structures and point group of main polyhedron of $M^{3+/4+}$-Ent(R/S) coordination atoms in MD simulations. The coordination atoms of Ent were colored by blue, purple, and orange, while the O_{water}-s are colored by red. CSAPR, SAPR, and TCTPR mean capped square antiprism, square antiprism, and tricapped trigonal prism stereochemistry structures, respectively.

	Ent(S)			Ent(R)		
		stereochemistry	point group		stereochemistry	point group
Fe^{3+}	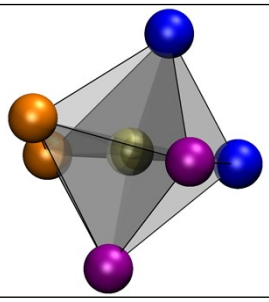	octahedron	O_h	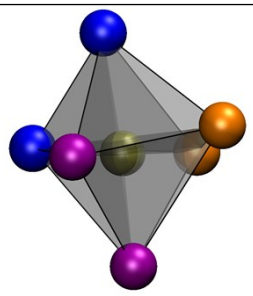	octahedron	O_h
Am^{3+}	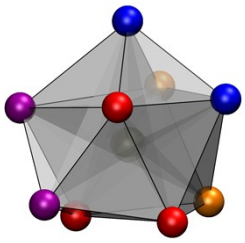	CSAPR	C_{4v}	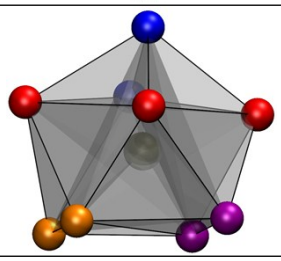	CSAPR	C_{4v}

	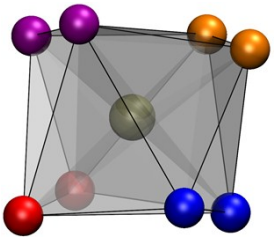	SAPR	D_{4d}	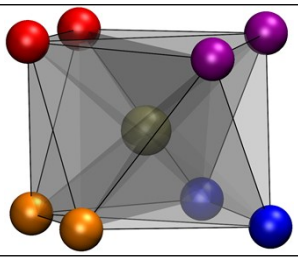	SAPR	D_{4d}
Cm^{3+}	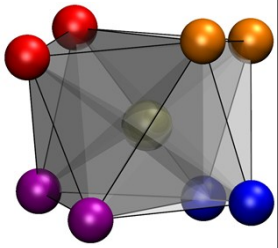	SAPR	D_{4d}	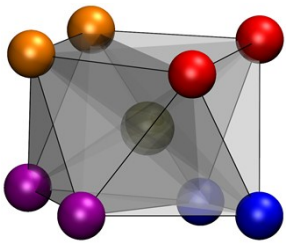	SAPR	D_{4d}
Th^{4+}	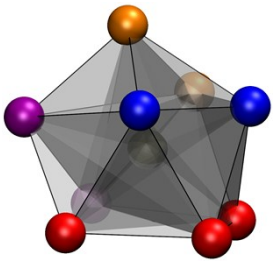	CSAPR	C_{4v}	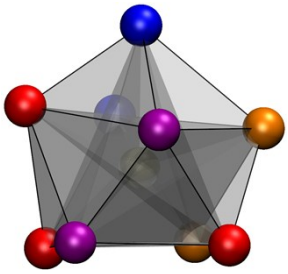	CSAPR	C_{4v}
				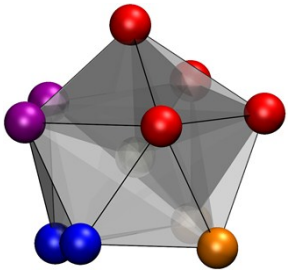	Bicapped dodecahedron	D_2
U^{4+}	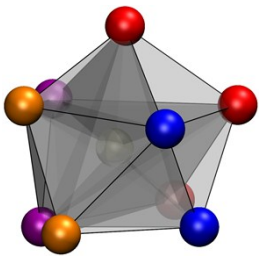	CSAPR	C_{4v}	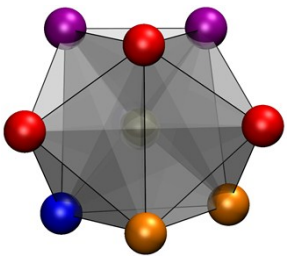	TCTPR	D_{3h}
				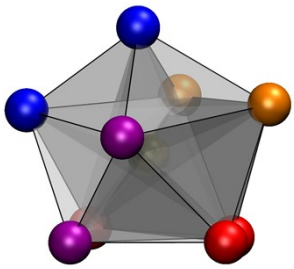	CSAPR	C_{4v}

Np^{4+}	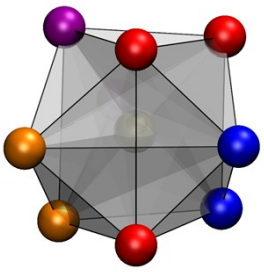	TCTPR	D_{3h}	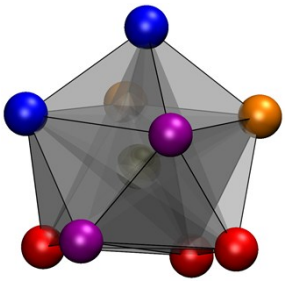	CSAPR	C_{4v}
	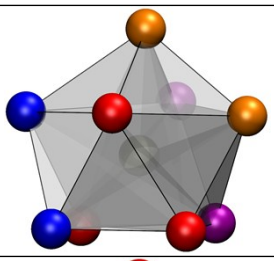	CSAPR	C_{4v}			
Pu^{4+}	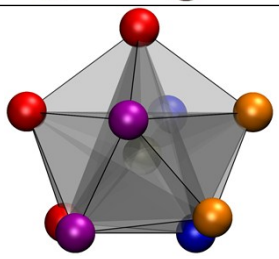	CSAPR	C_{4v}	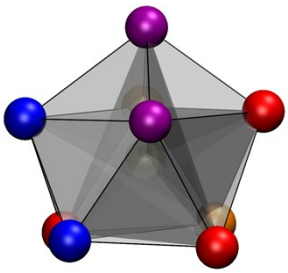	CSAPR	C_{4v}
	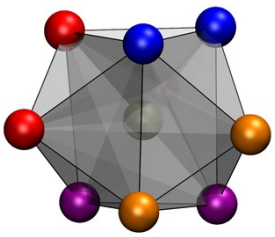	TCTPR	D_{3h}			

9. Evaluation of metal parameters

The force field parameters of the ions were validated before being used in the present study. In the validation (manuscript in preparation), since we could not find the experimental data of the actinide-Ent or actinide-catechol complexes, we have chosen several typical anions, i.e. Cl^-, NO_3^-, and CO_3^{2-}, which covered mono- and bidentate, mono- and dianionic ligands. The analysis of the conformation (coordination bond length, coordination number) of the complexes of actinides with water and the anions in aqueous phase displayed good agreement with available experimental data. We have also tested the parameters on the interactions between metal ions and deprotonated catechol anion

Below we tabulated the key properties of metal ion in water without (Table S8) and with the presence of ions Cl^-, NO_3^-, and CO_3^{2-} (Table S9), and deprotonated catechol (Table S10).

Table S8. The comparison of experimental values, 12-6-4 type simulated values in SPC/E water model and 12-6 IOD type simulated values in SPC/E water model of properties as IOD, CN, and HFE, respectively.

	Fe^{3+}	Am^{3+}	Cm^{3+}	Th^{4+}	U^{4+}	Np^{4+}	Pu^{4+}

IOD	Expt.	2.03[a]	2.48 [c]	2.46 [c]	2.45[a]	2.42[a]	2.40[d]	2.39[a]
	12-6-4 [b]	2.02[b]	/	/	2.45[b]	2.42[b]	/	2.39[b]
	12-6	1.99	2.48	2.46	2.43	2.39	2.39	2.37
CN	Expt.	6[a]	9 [e]	9 [e]	9-11[a]	9-11[a]	8-10 [e]	8[a]
	12-6-4 [b]	6.8[b]	/	/	10.0[b]	10.0[b]	/	10.0[b]
	12-6	6	9	9	9.9	9.1	9	9
HFE	Expt.	-1019.4[a]	-788.1 [f,] -764.3[g,] -755.0 [h]	-795.0[f], -778.0 [g], -770.8 [h]	-1389.8[a], -1457.9 [h]	-1567.9[a,] -1506.0 [h],	-1471.6 [g,] -1552.1 [h]	-1520.1[a,] -1540.2 [h],
	12-6-4 [b]	-1019.2[b]	/	/	-1388.3[b]	-1566.0[b]	/	-1520.3[b]
	12-6	-860.54	-712.35	-721.83	-1218.39	-1231.84	-1239.30	-1243.93
	12-6(corr)	-945.65	-782.80	-793.22	-1450.47	-1466.48	-1475.36	-1480.87

[a] data from Y. Marcus, *J. Chem. Soc., Faraday Trans.* 1991**,** *87* (18), 2995-2999.

[b] data from P. Li, L. F. Song and K. M. Merz Jr, *J. Phys. Chem. B*, 2014, **119**, 883-895.

[c] data from P. Allen, J. Bucher, D. Shuh, N. Edelstein, I. Craig, *Inorg. Chem.* 2000, **39**, 595-601.

[d] data from ref. P. G. Allen, J. J. Bucher, D. K. Shuh, N. M. Edelstein, T. Reich, *Inorg. Chem.* 1997, **36**, 4676-4683.

[e] data from P. R. Smirnov, V. N. Trostin, *Russian J. Gen. Chem.* 2012, **82**, 1204-1213.

[f] data from S. Goldman, L. R. Morss, *Can. J. Chem.* 1975, **53**, 2695-2700.

[g] data from F. H. David, *Radiochim. Acta* 2008, **96**, 135-144.

[h] data from F. H. David, V. Vokhmin, *New J Chem* 2003**,** *27* (11), 1627-1632.

Table S9. The coordination bond distance (Å) between actinide ion and coordinating atoms of Cl^-, NO_3^-, and CO_3^{2-} derived from calculated RDF over the 20 ns production run. Data in parenthesis are coordination numbers.

	Cl^-		NO_3^-		CO_3^{2-}	
	This work	Ref	This work	Ref	This work	ref
Th^{4+}	2.70(9.3)	2.72(10)[a]	2.30(9.2)	2.58(12)[c]	2.29(9.7)	2.50(10)[d]
U^{4+}	2.67(9)	2.63(6.0)[b]	2.27(9)	2.53(12)[e]	2.26(9)	2.49(10)[f]
Np^{4+}	2.66(9)	2.69(9.9)[g]	2.26(9)	2.52(11.5) [h]	2.23(9)	2.44(10)[i]
Pu^{4+}	2.64(9)	2.62(8)[a]	2.24(9)	2.39(10)[a]	2.21(9)	2.42(10)[j]
Am^{3+}	2.81(8.8)	2.80(8.8)[k]	2.42(8.8)	2.55(10)[l]	2.32(9)	--
Cm^{3+}	2.75(8.8)	2.76(8.7)[k]	2.40(8.8)	2.51(10)[l]	2.30(9)	2.34~2.42(9)[m]

[a] data from N. Kumar, J. M. Seminario, *J Phys Chem A* 2015**,** *119* (4), 689-703.

[b] data from B. Li, S. Dai, D. Jiang, *ACS Appl. Energy Mater.* 2019, *2* (3), 2122-2128.

[c] data from N. N. Rammo, K. R. Hamid, B. A. Khaleel, *J. Less Common Metals*, 1990, **162**, 1-9.

[d] data from A. R. Felmy, D. Rai, S. M. Sterner, M. J. Mason, N. J. Hess, S. D. Conradson, *J. Solution Chem.* 1997**,** *26* (3), 233-248.

[e] data from K. Takao, H. Kazama, Y. Ikeda, S. Tsushima, *Angew. Chem.* 2019, **131**, 246-249.

[f] data from C. Hennig, A. Ikeda-Ohno, F. Emmerling, W. Kraus, G. Bernhard, *Dalton T.*, 2010, **39**, 3744-3750

[g] data from P. G. Allen, J. Bucher, D. K. Shuh, N. M. Edelstein, T. Reich, *Inorg. Chem.*, 1997,

36, 4676-4683.

[h] data from A. Ikeda-Ohno, C. Hennig, A. Rossberg, H. Funke, A. C. Scheinost, G. Bernhard, T. Yaita, *Inorg. Chem.*, 2008, **47**, 8294-8305.

[i] data from M. S. Grigor'ev, N. A. Budantseva, A. M. Fedoseev, *Russ. J. Coord. Chem.*, 2013, **39**, 87-95.

[j] data from D. L. Clark, S. D. Conradson, D. W. Keogh, P. D. Palmer, B. L. Scott, C. D. Tait, *Inorg. Chem.*, 1998, **37**, 2893-2899.

[k] data from P. Allen, J. Bucher, D. Shuh, N. Edelstein, I. Craig, *Inorg. Chem.*, 2000, **39**, 595-601.

[l] data from S. M. Ali, S. Pahan, A. Bhattacharyya, P. K. Mohapatra, *Phys. Chem. Chem. Phys.*, 2016, **18**, 9816-9828.

[m] data from R. Spezia, Y. Jeanvoine, R. Vuilleumier, *J. Mol. Model.*, 2014, **20**, 2398.

Table S10. The IOD, CN values calculated from RDF results between Fe^{3+}/An^{3+}/An^{4+} and $O_{catechol}$, and O_{water}, and the M-catechol complex binding free energy at 310K and 1 atm. (Å for ion-oxygen-distance (IOD), kcal/mol for ΔG, respectively)

	Fe^{3+}	Am^{3+}	Cm^{3+}	Th^{4+}	U^{4+}	Np^{4+}	Pu^{4+}
IOD($O_{catechol}$)	1.86	2.32	2.32	2.28	2.26	2.24	2.22
CN($O_{catechol}$)	2.0	2.0	2.0	2.0	2.0	2.0	2.0
IOD(O_{water})	1.96	2.48	2.46	2.42	2.40	2.38	2.38
CN(O_{water})	4.0	7.0	7.0	7.3	7.1	7.0	7.0
CN(total)	6.0	9.0	9.0	9.3	9.1	9.0	9.0
ΔG_1	-900.79	-745.81	-751.73	-1277.43	-1292.35	-1301.33	-1305.95
ΔG_2	-863.17	-729.57	-735.04	-1242.07	-1253.40	-1262.03	-1266.39
ΔG_{bind}	-37.62	-16.24	-16.69	-35.36	-38.95	-39.30	-39.56
ΔG_{bind}(corr)	-41.34	-17.84	-18.34	-41.12	-45.29	-45.69	-46.00